Contents lists available at ScienceDirect

NJAS - Wageningen Journal of Life Sciences

C$_3$ and C$_4$ photosynthesis models: An overview from the perspective of crop modelling

X. Yin*, P.C. Struik

Centre for Crop Systems Analysis, Department of Plant Sciences, Wageningen University, P.O. Box 430, NL-6700 AK Wageningen, The Netherlands

ARTICLE INFO

ABSTRACT

Nearly three decades ago Farquhar, von Caemmerer and Berry published a biochemical model for C$_3$ photosynthetic rates (the FvCB model). The model predicts net photosynthesis (A) as the minimum of the Rubisco-limited rate of CO$_2$ assimilation (A_c) and the electron transport-limited rate of CO$_2$ assimilation (A_j). Given its simplicity and the growing availability of the required enzyme kinetic constants, the FvCB model has been used for a wide range of studies, from analysing underlying C$_3$ leaf biochemistry to predicting photosynthetic fluxes of ecosystems in response to global warming. However, surprisingly, this model has seen limited use in existing crop growth models. Here we highlight the elegance, simplicity, and robustness of this model. In the light of some uncertainties with photosynthetic electron transport pathways, a recently extended FvCB model to calculate A_j is summarized.

Applying the FvCB-type model in crop growth models for predicting leaf photosynthesis requires a stomatal conductance (g_s) model to be incorporated, so that intercellular CO$_2$ concentration (C_i) can be estimated. In recent years great emphasis has been put on the significant drawdown of Rubisco carboxylation-site CO$_2$ concentration (C_c) relative to C_i. To account for this drawdown, mesophyll conductance (g_m) for CO$_2$ transfer can be added. We present an analytical algorithm that incorporates a g_s model and uses g_m as a temperature-dependent parameter for calculating A under various environmental scenarios.

Finally we discuss a C$_4$-equivalent version of the FvCB model. In addition to the algorithms already elaborated for C$_3$ photosynthesis, most important algorithms for C$_4$ photosynthesis are those that capture the CO$_2$ concentrating mechanism and the extra ATP requirement by the C$_4$ cycle. Although the current estimation of the C$_4$ enzyme kinetic constants is less certain, applying FvCB-type models to both C$_3$ and C$_4$ crops is recommended to accurately predict the response of crop photosynthesis to multiple, interactive environmental variables.

© Published by Elsevier B.V. on behalf of Royal Netherlands Society for Agricultural Sciences.

1. Introduction

Photosynthesis is the primary physiological process that drives plant growth and crop productivity and influences many other plant processes. It is also strongly affected by environmental stresses. Its study becomes increasingly important in the context of assessing the impact of climate change on agro-ecosystem function and of exploring opportunities for bio-based energy production. Therefore, mechanistic quantification of photosynthesis deserves further attention in dynamic simulation models of crop growth (crop growth models hereafter).

Photosynthesis is one of the most studied and best understood physiological processes. In the wake of the advent of the systems biology era, detailed biochemical models of photosynthesis, comprising its light reactions, electron and proton transport, enzymatic reactions, and regulatory functions, have been recently developed (e.g., [1,2]). These models are very useful for any transient, kinetic investigation of photosynthesis in response to environmental variables. Because of their complexity and required short time resolution, however, these models are unsuitable for use as a leaf-level model for large-scale modelling of photosynthesis of crop canopies or vegetation. The biochemical model for C$_3$ photosynthetic CO$_2$ assimilation published by Farquhar, von Caemmerer and Berry [3] (the FvCB model hereafter) makes no attempt to model all the processes of photosynthesis from light harvesting to metabolism but rather simplifies, summarizes and synthesizes the knowledge of the contributing mechanisms by focusing on a few key processes. Because of its excellent performance given its simplicity [4], and the growing availability of the required enzyme kinetic constants (e.g., [5,6]), the FvCB model has been used for a

* Corresponding author.
  E-mail address: xinyou.yin@wur.nl (X. Yin).

wide range of studies, from analysing underlying C_3 leaf biochemistry (e.g., [4]) to predicting photosynthetic fluxes of ecosystems in response to global environmental change (e.g., [7,8]). However, this model has seen very limited use in crop growth models.

Our objective is to 'catalyse' the use of the FvCB model by the crop modelling community. To this end, we shall (1) high-

light the elegance, simplicity, and robustness of the model, (2) summarize an extended FvCB model that addresses some uncertainties with photosynthetic electron (e^-) transport pathways, and (3) discuss the mathematical coupling of the FvCB model with CO_2-diffusional conductance models so that the value of A (see Table 1 for model variable definition) can be modelled for any

Table 1
List of main variables used in the models and their units.

Variable	Definition	Unit
a_1	An empirical coefficient, see Eq. (15a)	–
A	Net photosynthesis rate	μmol CO_2 m^{-2} s^{-1}
A_c	Rubisco activity limited net photosynthesis rate	μmol CO_2 m^{-2} s^{-1}
A_j	Electron transport limited net photosynthesis rate	μmol CO_2 m^{-2} s^{-1}
b_1	An empirical coefficient, see Eq. (15a)	kPa^{-1}
C_a	Ambient air CO_2 partial pressure	μbar or μmol mol^{-1}
C_c	Chloroplast CO_2 partial pressure	μbar
C_i	Intercellular CO_2 partial pressure	μbar
C_{i*}	C_i-based CO_2 compensation point in the absence of R_d	μbar
C_s	Leaf-surface CO_2 partial pressure	μbar
C_{s*}	C_s-based CO_2 compensation point in the absence of R_d	μbar
D	Deactivation energy	J mol^{-1}
E	Activation energy	J mol^{-1}
f_{cyc}	Fraction of electrons at PSI that follow cyclic transport around PSI	–
f_{pseudo}	Fraction of electrons at PSI that follow pseudocyclic transport	–
f_Q	Fraction of electrons at reduced plastoquinone that follow the Q-cycle	–
f_{vpd}	Factor for describing the effect of leaf-to-air vapour difference on g_s	–
g_0	Residual stomatal conductance when irradiance approaches zero	mol m^{-2} s^{-1} bar^{-1}
g_b	Boundary-layer conductance	mol m^{-2} s^{-1} bar^{-1}
g_{bs}	Bundle-sheath conductance	mol m^{-2} s^{-1} bar^{-1}
g_m	Mesophyll diffusion conductance	mol m^{-2} s^{-1} bar^{-1}
g_s	Stomatal conductance	mol m^{-2} s^{-1} bar^{-1}
h	Number of protons required to produce one ATP	mol mol^{-1}
I_{abs}	Photon flux density absorbed by leaf photosynthetic pigments	μmol photon m^{-2} s^{-1}
I_{inc}	Photon flux density incident to leaves	μmol photon m^{-2} s^{-1}
J	Rate of e^- transport	μmol e^- m^{-2} s^{-1}
J_2	Rate of all e^- transport through PSII	μmol e^- m^{-2} s^{-1}
J_{max}	Maximum value of J under saturated light	μmol e^- m^{-2} s^{-1}
J_{2max}	Maximum value of J_2 under saturated light	μmol e^- m^{-2} s^{-1}
k_p	Initial carboxylation efficiency of the PEP carboxylase	mol m^{-2} s^{-1} bar^{-1}
K_{mC}	Michaelis–Menten constant of Rubisco for CO_2	μbar
K_{mO}	Michaelis–Menten constant of Rubisco for O_2	μbar
L	Leak rate of CO_2 out of the bundle sheath	μmol CO_2 m^{-2} s^{-1}
O	Oxygen partial pressure	μbar
O_i	Intercellular oxygen partial pressure	μbar
O_{bs}	Bundle-sheath oxygen partial pressure	μbar
P_{max}	Maximum gross photosynthetic rate under saturated irradiance	μmol CO_2 m^{-2} s^{-1}
R	Universal gas constant (=8.314)	J K^{-1} mol^{-1}
R_d	Day respiration (respiratory CO_2 release other than by photorespiration)	μmol CO_2 m^{-2} s^{-1}
R_m	Day respiration in the mesophyll	μmol CO_2 m^{-2} s^{-1}
s	A lumped parameter, equal to $\rho_2\beta[1-f_{pseudo}/(1-f_{cyc})]$	–
S	Entropy term	J K^{-1} mol^{-1}
$S_{c/o}$	Relative CO_2/O_2 specificity factor for Rubisco	bar bar^{-1}
T	Leaf temperature	°C
V_{cmax}	Maximum rate of Rubisco activity-limited carboxylation	μmol CO_2 m^{-2} s^{-1}
V_p	PEP carboxylation rate	μmol CO_2 m^{-2} s^{-1}
$V_p(J_2)$	e^- transport-limited PEP carboxylation rate	μmol CO_2 m^{-2} s^{-1}
V_{pmax}	Maximum PEP carboxylation rate	μmol CO_2 m^{-2} s^{-1}
x	Fraction of PSII e^- transport rate partitioned to the C_4 cycle	–
z	A lumped parameter, equal to $(2+f_Q-f_{cyc})/[h(1-f_{cyc})]$	mol mol^{-1}
α	Fraction of PSII activity in the bundle sheath	–
$\alpha_{(LL)}$	Conversion efficiency of absorbed light into J at strictly limiting light	mol e^- (mol photon)$^{-1}$
$\alpha_{2(LL)}$	Quantum efficiency of PSII e^- transport under strictly limiting light, on the combined PSI- and PSII-absorbed light basis	mol e^- (mol photon)$^{-1}$
β	Absorptance by leaf photosynthetic pigments	–
γ_*	Half of the reciprocal of $S_{c/o}$	bar bar^{-1}
$\kappa_{2(LL)}$	Conversion efficiency of incident light into J at strictly limiting light	mol e^- (mol photon)$^{-1}$
θ	Convexity factor for response of J to irradiance	–
θ_2	Convexity factor for response of J_2 to absorbed light	–
ρ_2	Proportion of absorbed light partitioned to PSII	–
$\Phi_{1(LL)}$	Quantum efficiency of PSI e^- flow at the strictly limiting light level	mol e^- (mol photon)$^{-1}$
Φ_2	Quantum efficiency of PSII e^- flow on PSII-absorbed light basis	mol e^- (mol photon)$^{-1}$
$\Phi_{2(LL)}$	Value of Φ_2 at the strictly limiting light level	mol e^- (mol photon)$^{-1}$
$\Phi_{CO_2(LL)}$	Quantum efficiency of CO_2 assimilation at strictly limiting light	mol CO_2 (mol photon)$^{-1}$
Γ	C_c- or C_i-based CO_2 compensation point in the presence of R_d	μbar
Γ_*	C_c-based CO_2 compensation point in the absence of R_d	μbar

environmental scenario. Finally, we shall describe and discuss an equivalent, combined model for C_4 photosynthesis and conductance, building upon previous C_4 photosynthesis models, e.g., as described by von Caemmerer and Furbank [9].

2. The Farquhar, von Caemmerer and Berry model

The FvCB model predicts A as the minimum of the Rubisco-limited rate of CO_2 assimilation (A_c) and the electron transport-limited rate of CO_2 assimilation (A_j):

$$A = \min(A_c, A_j) \tag{1}$$

An illustration of the two parts of limitations along the CO_2-response curves is given in Fig. 1. Sharkey et al. [10] have drawn attention to a third limitation by triose phosphate utilization, which is not discussed here because it comes into play only occasionally at very high CO_2 levels.

The value of A_c is calculated as a function of the maximum carboxylation capacity of Rubisco (V_{cmax}) by:

$$A_c = \frac{(C_c - \Gamma_*)V_{c\,max}}{C_c + K_{mC}(1 + O/K_{mO})} - R_d \tag{2}$$

where C_c is the CO_2 partial pressure at the carboxylating sites of Rubisco, K_{mC} and K_{mO} are Michaelis–Menten constants of Rubisco for CO_2 and O_2, respectively, and Γ_* is the CO_2 compensation point in the absence of day respiration (R_d).

In the calculation of A_j, the FvCB model assumes 100% non-cyclic e^- transport, thus excluding cyclic e^- transport around PSI (CET). There are two widely used forms of the equation for electron transport-limited rate of photosynthesis:

$$A_j = \frac{(C_c - \Gamma_*)J}{4C_c + 8\Gamma_*} - R_d \tag{3a}$$

$$A_j = \frac{(C_c - \Gamma_*)J}{4.5C_c + 10.5\Gamma_*} - R_d \tag{3b}$$

The relationship between e^- transport rate (J) in Eqs. (3a), (3b) and irradiance was first described as a rectangular hyperbola [11], using quantum yield of e^- transport under limiting light ($\alpha_{(LL)}$) and the maximum capacity of e^- transport (J_{max}). Following Farquhar and Wong [12], most applications of the FvCB model, however,

Fig. 1. An idealized curve for the response of net CO_2 assimilation rate (A) in C_3 plants to intercellular CO_2 partial pressure (C_i), in which 12 data points are shown. Points 1–6 locate within the range of the Rubisco-limited rate (A_c) whereas points 7–12 are within the range of electron transport-limited rate (A_j). The portions of each curve without data points are the extended parts as given by the A_c and A_j equation, respectively. The minimum of A_c and A_j gives the modelled CO_2 response curve as indicated by the 12 data points.

describe J as a non-rectangular hyperbolic function of irradiance by:

$$J = \frac{\left(\alpha_{(LL)}I_{abs} + J_{max} - \sqrt{(\alpha_{(LL)}I_{abs} + J_{max})^2 - 4\theta J_{max}\alpha_{(LL)}I_{abs}}\right)}{2\theta} \tag{4}$$

where θ is the convexity of the response curve of J to light absorbed by photosynthetic pigments (I_{abs}). Equations like Eq. (4) that describe the light response of e^- transport rate mimic well the photosynthetic down-regulation induced by high light levels via mechanisms such as non-photochemical quenching and chloroplast avoidance movement [13]. The theoretical maximum value for $\alpha_{(LL)}$ is 0.5 mol electron per mol photon absorbed [3] because one quantum must be absorbed by each of the two photosystems to move an electron from the level of H_2O to that of $NADP^+$. However, in actual applications (e.g., [14–17]), $\alpha_{(LL)}$ has been empirically adjusted to a lower value to agree with a measured quantum efficiency for CO_2 uptake that is often lower than that expected from the theoretical maximum.

The temperature dependence of R_d and kinetic properties of Rubisco (involving three parameters V_{cmax}, K_{mC} and K_{mO}) in Eq. (2) is described by an Arrhenius function normalized with respect to their values at 25 °C:

$$\text{Parameter} = \text{Parameter}_{25}e^{(T-25)E/[298R(T+273)]} \tag{5}$$

where T is leaf temperature; E is the activation energy, defining the responsiveness of the relevant parameter to temperature; R is the universal gas constant. A modified Arrhenius function is used to describe the optimum response of other parameters (e.g., J_{max}) to temperature as [17]:

$$\text{Parameter} = \text{Parameter}_{25}e^{(T-25)E/[298R(T+273)]}$$
$$\times \frac{1 + e^{(298S-D)/(298R)}}{1 + e^{[(T+273)S-D]/[R(T+273)]}} \tag{6}$$

where S is an entropy term; E and D are the energies of activation and deactivation, defining the responsive shape of the sub- and supra-optimal ranges, respectively. June et al. [18] described an alternative, simpler equation for this optimum response. It may be argued that these response equations lack a mechanistic basis since parameters such as E are often estimated from fitting to experimental data [17,19]. However, the equations do provide a flexibility to accommodate possible variability in the shape of the temperature response, e.g., among genotypes or species.

The value Γ_* depends on the O_2 concentration (O) and the Rubisco CO_2/O_2 specificity factor ($S_{c/o}$) as follows:

$$\Gamma_* = \frac{0.5O}{S_{c/o}} \tag{7}$$

where the factor 0.5 is mol CO_2 released when Rubisco catalyses the reaction with 1 mol O_2 in photorespiration [3]. The value of $S_{c/o}$, which also depends on temperature and can be described by Eq. (5) in which E should be negative to account for a decline of the Rubisco affinity for CO_2 with increasing temperature.

The values of V_{cmax} and J_{max} depend on the concentration of relevant enzymes. For practical purposes, V_{cmax25} and J_{max25} increase linearly with leaf nitrogen content (e.g., [14,20]). Other parameters are assumed constant, and their in vivo estimates are shown in Table 2.

The basic equations of the FvCB model, Eqs. (1)–(4), capture the response of C_3 photosynthesis to irradiance, CO_2 and O_2 levels, although the model may not predict often observed increases in the initial slope of the photosynthetic response curve to CO_2 with increased light levels (e.g., [21,22]). Coupled with auxiliary equations, Eqs. (5)–(7) and the linear relation between leaf nitrogen level and V_{cmax25} or J_{max25} (e.g., [14,16,23,24]), the model also

Table 2
Indicative values for constants used in the C_3 and C_4 photosynthesis models.

Constant	Unit	C_3		C_4	
		Value	Reference	Value	Reference
$S_{c/o25}$	bar bar^{-1}	2800	Bernacchi et al. [6]	2590	von Caemmerer [54]
K_{mC25}	μbar	270	Bernacchi et al. [6]	650	von Caemmerer [54]
K_{mO25}	μbar	165000	Bernacchi et al. [6]	450000	von Caemmerer [54]
$E_{Sc/o}$	J mol^{-1}	–24460	Bernacchi et al. [6]	?	
E_{Vcmax}	J mol^{-1}	65330	Bernacchi et al. [71]	67300	Massad et al. [53]
E_{KmC}	J mol^{-1}	80990	Bernacchi et al. [6]	?	
E_{KmO}	J mol^{-1}	23720	Bernacchi et al. [6]	?	
E_{Rd}	J mol^{-1}	46390	Bernacchi et al. [71]	?	
E_{Jmax}	J mol^{-1}	26900–94400	Yin et al. [19]	77900	Massad et al. [53]
D_{Jmax}	J mol^{-1}	200000	Medlyn et al. [17]	192000	Massad et al. [53]
S_{Jmax}	J K^{-1} mol^{-1}	650	Harley et al. [14]	630	Massad et al. [53]
E_{Vpmax}	J mol^{-1}	na		70400	Massad et al. [53]
D_{Vpmax}	J mol^{-1}	na		118000	Massad et al. [53]
S_{Vpmax}	J K^{-1} mol^{-1}	na		380	Massad et al. [53]
E_{gm}	J mol^{-1}	49600	Bernacchi et al. [6]	na	
D_{gm}	J mol^{-1}	437400	Bernacchi et al. [6]	na	
S_{gm}	J K^{-1} mol^{-1}	1400	Bernacchi et al. [6]	na	
k_p	mol m^{-2} s^{-1} bar^{-1}	na		0.7	Collatz et al. [51]
θ, or θ_2	–	0.7 or	von Caemmerer [54]	0.7	von Caemmerer [54]
	–	variable	Bernacchi et al. [38]		
s	–	0.33–0.41	Yin et al. [20]	na	
$\Phi_{1(LL)}$	mol mol^{-1}	0.95–1.0	Trissl and Wilhelm [36]	0.95–1.0	Kingston-Smith et al. [72]
$\Phi_{2(LL)}$	mol mol^{-1}	≈ 0.75	Yin et al. [20]	≈ 0.75	Assumed as C_3 value
β	–	0.84 or variable	Standard value in Li-Cor, Evans [73]	0.84	Standard value in Li-Cor
h	mol mol^{-1}	3, 4, 14/3	Yin et al. [70]	3 or 4	von Caemmerer [54]
x	–	na		0.4	von Caemmerer [54]
f_{pseudo}	–	≈ 0.1	Yin et al. [35]	≈ 0.1	Laisk and Edwards [59]
f_Q	–	0–1	von Caemmerer [54]	1	Furbank et al. [56]
a_1	–	≈ 0.85	†	≈ 0.85	†
b_1	kPa^{-1}	≈ 0.14	†	≈ 0.20	†

?: not known to the authors; and their values for C_3 leaves are used tentatively here for simulation. na: not applicable. (†) Derived here from the data of Morison and Gifford [74].

quantifies the photosynthetic responses to temperature and nitrogen level. Putting all together, the responses of photosynthesis to these environmental variables can be unambiguously predicted mechanistically by the model.

CO_2 exchange at the leaf level can now be measured routinely with commercially available equipment [25] such as the Li-Cor 6400 (Li-Cor Inc., Lincoln, NE, USA). With such measurements, parameters of the FvCB model can be estimated using nonlinear regression fitting (e.g., [14,17,19,26–28]), especially when CO_2 exchange measurements are combined with chlorophyll fluorescence measurements [20].

Leaf photosynthesis in crop growth simulation has traditionally been calculated using a family of empirical equations for its light response curves. Typically these curves are characterized by two parameters: initial quantum use efficiency of CO_2 assimilation at limiting lights ($\Phi_{CO_2(LL)}$) and maximum gross CO_2 assimilation rate under a saturating light (P_{max}). Empirical calibration procedures are needed if the models are used to predict the effect of environmental variables other than light on photosynthesis. According to van Oijen et al. [29], both $\Phi_{CO_2(LL)}$ and P_{max} can be formulated from the FvCB model:

$$\Phi_{CO_2(LL)} = \frac{\alpha_{(LL)}(C_c - \Gamma_*)}{4.5C_c + 10.5\Gamma_*} \qquad (8)$$

$$P_{max} = \frac{(C_c - \Gamma_*)V_{c\,max}}{C_c + K_{mC}(1 + O/K_{mO})} \qquad (9)$$

where Eq. (8) holds if Eq. (3b) applies; if Eq. (3a) applies, the coefficients 4.5 and 10.5 should be replaced by 4 and 8, respectively. Eq. (9) holds in general, but according to the FvCB model, P_{max} can sometimes be determined as $(A_j + R_d)$ rather than $(A_c + R_d)$, as done by Boote and Pickering [30]. When Eqs. (8) and (9) are used there

is no need to conduct empirical model calibrations or corrections for a change in environmental conditions such as CO_2 concentration. Note that empirical calibrations were implemented in some crop growth models, e.g., the rice model ORYZA ([31]; see a later section).

Observed temperature response curves of photosynthesis under various CO_2 or light levels (e.g., [32]) provide strong support for the FvCB model, although uncertainties may exist for the modelled response over the range of low temperatures down to 0 °C. This model predicts that at high CO_2 levels the rate of photorespiration is reduced, thereby extending the temperature range where CO_2 assimilation rate is positive. The model also predicts an increasing and more pronounced temperature optimum with increasing either CO_2 or light levels (Fig. 2). Such a shift in the temperature optimum with a change in other environmental factors is critically important for correctly assessing the impact of climate change [7], e.g., on crop production and agro-ecosystem functioning. However, such interactions of temperature with light or CO_2 levels cannot be predicted by any empirical photosynthesis models using a simple light response equation.

3. An extended model and its use for calibrating the Farquhar, von Caemmerer and Berry model

There is, however, an ambiguity in the FvCB model for calculating A_j, as shown by the use of two equations—Eqs. (3a) and (3b). In applying the FvCB model, some researchers (e.g., [14]) have used Eq. (3a), whereas others (e.g., [7]) used Eq. (3b), with little explanation why one form was preferred over the other. Eqs. (3a) and (3b) were derived by assuming that the noncyclic e$^-$ transport was the only photosynthetic e$^-$ transport process active in leaves. This assumption results in two possible outcomes: either the NADPH or the ATP
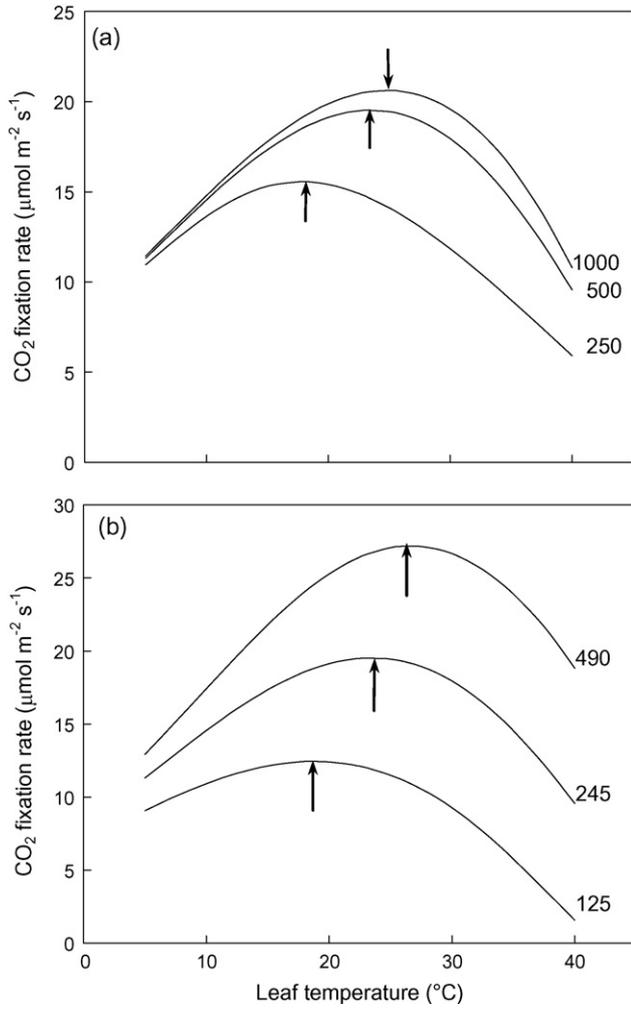
Fig. 2. An example of response curves of net CO_2 assimilation rate in a C_3 plant to leaf temperature, modelled using the FvCB model, (a) at three levels of irradiance ($\mu mol\,m^{-2}\,s^{-1}$) when C_c was fixed at 245 μbar, and (b) at three levels of C_c (μbar) when irradiance was fixed at 500 $\mu mol\,m^{-2}\,s^{-1}$. Arrows indicate the position of the optimum temperature.

supply will limit overall photosynthesis, applying to Eq. (3a) and Eq. (3b), respectively. Furthermore, Eq. (3a) assumes 100% linear e⁻ transport (LET), the noncyclic e⁻ flux used for carbon reduction and photorespiration. Eq. (3b) implies that in addition to the LET there is some pseudocyclic e⁻ transport (PET), the noncyclic e⁻ flux not used for carbon reduction and photorespiration. Comparing Eqs. (3a) and (3b) indicates that ATP production is more limiting than NADPH supply. Thus, in Eq. (3b), PET is assumed to occur *in vivo* to reduce or eliminate the ATP deficit.

Many studies (e.g., [14,15]) in which the FvCB model was applied calculated e⁻ transport rate (J) using a constant quantum yield of e⁻ transport, which is usually corrected empirically for the observed $\Phi_{CO_2(LL)}$. In fact, $\Phi_{CO_2(LL)}$ is a function of excitation partitioning of absorbed light between photosystem I (PSI) and photosystem II (PSII), and e⁻ transfer efficiencies of PSI and PSII. Furthermore, any involvement of CET will reduce observed $\Phi_{CO_2(LL)}$. To account for the fraction of CET (f_{cyc}) and PET (f_{pseudo}) (Fig. 3) as well as for the difference between PSI and PSII e⁻ transport efficiencies under limiting light ($\Phi_{1(LL)}$ and $\Phi_{2(LL)}$, respectively) and for an uncertainty with regard to the operation of the Q-cycle (f_Q) and the protons required for synthesising one mol ATP (h), the FvCB model for A_j was extended analytically for a generalized stoichiometry ([19,35])

by:

$$A_j = J_2 \left(1 - \frac{f_{pseudo}}{1 - f_{cyc}}\right) \frac{C_c - \Gamma_*}{4C_c + 8\Gamma_*} - R_d \tag{10a}$$

$$J_2 = \frac{\left(\alpha_{2(LL)}I_{abs} + J_{2\,max} - \sqrt{(\alpha_{2(LL)}I_{abs} + J_{2\,max})^2 - 4\theta_2 J_{2\,max}\alpha_{2(LL)}I_{abs}}\right)}{2\theta_2} \tag{10b}$$

$$\alpha_{2(LL)} = \frac{\Phi_{2(LL)}(1 - f_{cyc})}{\Phi_{2(LL)}/\Phi_{1(LL)} + (1 - f_{cyc})} \tag{10c}$$

$$1 - f_{cyc} - f_{pseudo} = \frac{(4C_c + 8\Gamma_*)(2 + f_Q - f_{cyc})}{h(3C_c + 7\Gamma_*)} \tag{10d}$$

where J_2 is e⁻ transport rate through PSII while CET is running simultaneously, θ_2 is the convexity of the response curve of J_2 to I_{abs}, and J_{2max} is the maximum capacity of J_2 under a saturating I_{abs}. Eq. (10d) sets the requirement for the relation between f_{cyc}, f_{pseudo} and f_Q if ATP and NADPH produced in the thylakoid reactions are to match the requirement by the carbon reduction cycle and photorespiration. As shown by Yin et al. [19], Eqs. (3a) and (3b) of the FvCB model are special cases of the extended model assuming the lack of CET (i.e., $f_{cyc} = 0$) and an h of 3, with either no (Eq. (3b)) or only a small fraction (Eq. (3a)) of the electrons following the Q-cycle. Contemporary literature (e.g., [33,34]) indicates an h of 4 or even higher, coupled with the absolute operation of the Q-cycle (i.e., $f_Q = 1$).

Yin et al. [35] discussed how the extended model can be used to theoretically infer the possible range of variation for values of f_{cyc} and f_{pseudo} based on gas exchange measurements on $\Phi_{CO_2(LL)}$ and biophysical measurements on $\Phi_{1(LL)}$ and $\Phi_{2(LL)}$. The model can also calculate theoretically the value of ρ_2, the fraction of absorbed light partitioned to PSII, conditional to f_{cyc} and PSI and PSII e⁻ transport efficiencies. Furthermore, parameter $\alpha_{(LL)}$ in the FvCB model may be calculated as $\Phi_{2(LL)}/(1 + \Phi_{2(LL)}/\Phi_{1(LL)})$, derived from Eq. (10c) for the case in the absence of CET. This allows $\alpha_{(LL)}$ in the FvCB model to be calculated from biophysical measurements for a difference in e⁻ transport efficiency between PSI and PSII. The absolute maximum efficiency of PSI e⁻ transport is 0.95 or greater [36]. Chlorophyll fluorescence measurements showed that the maximum PSII photochemical efficiency for dark-adapted leaves was quite conservative among plant species, about 0.83 [37]. However, Bernacchi et al. [38] and Yin et al. [20] have shown that the equivalent efficiency for leaves adapted to strictly limiting light is somewhat lower, ca. 0.75. Setting $\Phi_{1(LL)} = 1$ and $\Phi_{2(LL)} = 0.75$ gives $\alpha_{(LL)}$ in the FvCB model as $\Phi_{2(LL)}/(1 + \Phi_{2(LL)}/\Phi_{1(LL)}) = 0.43$. This potentially avoids an empirical calibration for parameter $\alpha_{(LL)}$ in applying the FvCB model.

However, the estimation of $\alpha_{(LL)}$ for the FvCB model in that way is correct only if alternative e⁻ transports (PET and CET) do not occur, which is highly unlikely in leaves. By comparing Eq. (3a) with Eq. (10a), the following equation can be derived:

$$J = J_2 \left(1 - \frac{f_{pseudo}}{1 - f_{cyc}}\right) = \rho_2 \beta I_{inc} \Phi_2 \left(1 - \frac{f_{pseudo}}{1 - f_{cyc}}\right) = sI_{inc}\Phi_2 \tag{11}$$

where $s = \rho_2\beta[1 - f_{pseudo}/(1 - f_{cyc})]$, with β being the proportion of incident light absorbed by photosynthetic pigments. Although values of β, ρ_2, f_{cyc} and f_{pseudo} may be variable, they can be practically assumed independent of light levels, as done in many physiological studies. So the lumped parameter s can also be considered as constant. Substituting Eq. (11) into Eq. (3a) gives:

$$A_j = \frac{(C_c - \Gamma_*)sI_{inc}\Phi_2}{4C_c + 8\Gamma_*} - R_d \tag{12}$$
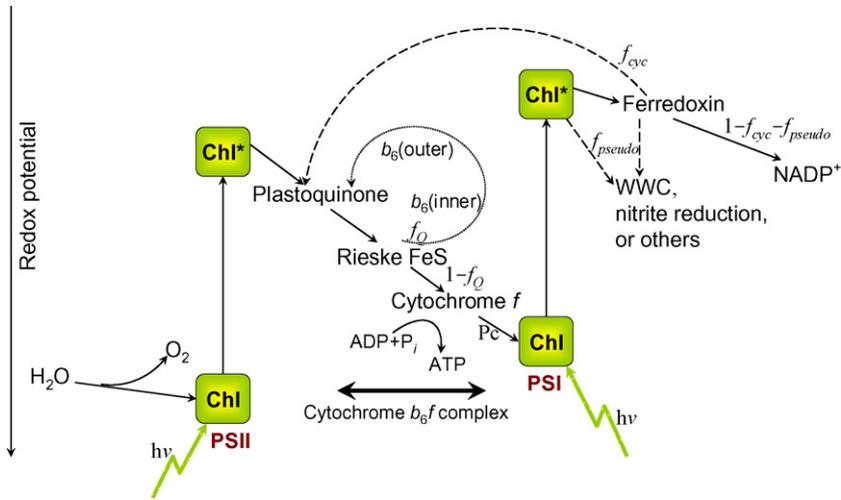
Fig. 3. The *Z* scheme for photosynthetic thylakoid reactions showing linear (solid arrows), cyclic and pseudocyclic (dashed arrows) electron transport routes. From reduced ferredoxin, a fraction, f_{cyc}, of the electrons follows the cyclic mode around PSI. Another fraction, f_{pseudo}, of the electrons that have passed PSI follows the pseudocyclic mode for supporting processes such as the water–water cycle (WWC, see [69]), or nitrite reduction, or other minor metabolic processes. The remaining fraction, $1 - f_{cyc} - f_{pseudo}$, is transferred to $NADP^+$—the terminal acceptor of the linear electron transport for generating NADPH in support of CO_2 reduction or photorespiration. The efficiency of ATP synthesis along the chain depends on the operation of the Q-cycle. The scheme shows that a fraction, f_Q, of the electrons followed the Q-cycle (dotted arrow) through the concerted action of the Rieske FeS and b_6 of the cytochrome b_6f complex, and the remaining fraction, $1 - f_Q$, is transferred directly towards plastocyanin (Pc). Chl, chlorophyll; $h\nu$, photons absorbed either by PSI or by PSII. Redrawn from Yin et al. [70].

Combined measurements of CO_2 exchange and chlorophyll fluorescence over the range (e.g., low light and high CO_2 levels) where *A* is limited by A_j, could be used to determine the value of *s*, that is, as the slope of linear regression, based on Eq. (12), between *A* and $I_{inc}\Phi_2/4$, obtained under the non-photorespiratory condition (low O_2 and/or high CO_2), at which Γ_* can be practically set to zero [20].

If parameter *s* is known, the efficiency for converting I_{inc} into LET under the strictly limiting light condition, $\kappa_{2(LL)}$, is given by:

$$\kappa_{2(LL)} = s\Phi_{2(LL)} \tag{13}$$

In analogy to Eq. (4), the equation for calculating *J* but as a function of incident irradiance can then be established as:

$$J = \frac{\left(\kappa_{2(LL)}I_{inc} + J_{max} - \sqrt{(\kappa_{2(LL)}I_{inc} + J_{max})^2 - 4\theta J_{max}\kappa_{2(LL)}I_{inc}}\right)}{2\theta} \tag{14}$$

Then, A_j could still be calculated by Eq. (3a), with *J* being given by Eq. (14). This way of calibration accounts for any occurrence of alternative e^- transport. An advantage of using Eq. (14) with parameter $\kappa_{2(LL)}$ over Eq. (4) is that parameter $\kappa_{2(LL)}$ can be determined from combined measurements of gas exchange and chlorophyll fluorescence without the necessity to measure parameter β, which is very hard to measure and is often approximated by total leaf absorptance (note that there is probably significant absorptance by non-photosynthetic pigments in leaves). With this calibration procedure, only a single lumped parameter $\kappa_{2(LL)}$ is needed, obviating the need for knowing individual underlying parameters β, ρ_2, f_{cyc} and f_{pseudo}, which would need more detailed measurements to estimate specifically. Yin et al. [20] showed for wheat leaves, that $\kappa_{2(LL)}$ can be related to leaf nitrogen (N) content (in $g\,m^{-2}$) as: $\kappa_{2(LL)} = 0.2048 + 0.0435N$. So, if no chlorophyll fluorescence or non-photorespiratory measurements were conducted for performing the aforementioned calibration procedure, $\kappa_{2(LL)}$ can be first derived practically using this equation.

4. Coupled modelling of C₃ photosynthesis and diffusional conductance

The FvCB-type models, in principle, require C_c to be known *a priori*, although Farquhar et al. [3] initially used the intercellular

CO_2 level (C_i) in places of C_c of Eqs. (2) and (3a), (3b). Diffusional conductance (including boundary-layer, stomatal and mesophyll components) is involved along the path of transfer from ambient CO_2 level (C_a) to C_c (Fig. 4). The first two components determine the drawdown of C_i relative to C_a. Of the three components, stomatal conductance (g_s) was formerly considered as most important, so in applying the FvCB model, C_i was then being treated as equal to C_c (e.g., [16]). In recent years, mesophyll conductance (g_m) for CO_2 transfer has increasingly been found to be small enough for the existence of a significant drawdown of C_c relative to C_i (see the review of [39]). As it is the level of C_c rather than C_i that together
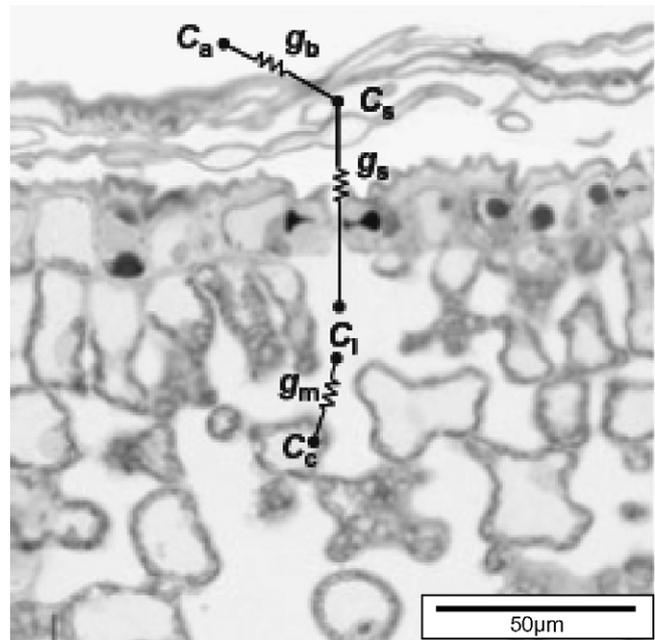
Fig. 4. Micrograph of the abaxial surface of a typical leaf, illustrating the pathway of CO_2 transfer from ambient air (C_a) through leaf surface (C_s) and intercellular air spaces (C_i) to the Rubisco carboxylation-sites in chloroplasts (C_c). Boundary-layer conductance (g_b), stomatal conductance (g_s), and mesophyll conductance (g_m) are indicated. Revised from Flexas et al. [39].

with the oxygen level determines the relative Rubisco activity for CO_2 fixation, g_m has to be incorporated into the FvCB model. A number of methods have been developed to estimate g_m [40–42]. The estimated g_m appears to respond to temperature [6,43,44] and this response may be described by Eq. (6) [6]. It has been shown recently that g_m may also vary with CO_2 and irradiance [45,39,20], but this variation is not yet completely certain (see review of [41] and references therein). Thus, we currently assume that g_m does not vary with CO_2 or with irradiance.

A coupled modelling of leaf photosynthesis and stomatal conductance has been reported frequently in the literature (e.g., [16,46]). Few whole-plant modelling studies have considered g_m as a necessary term of the photosynthesis models [39]. Here we incorporate g_b (boundary-layer conductance), g_s and g_m into our modelling framework. First, on the basis of several existing models, we propose the following phenomenological sub-model for g_s:

$$g_s = g_0 + \frac{A + R_d}{C_i - C_{i*}} f_{vpd} \qquad (15)$$

where g_0 is the residual stomatal conductance if the irradiance approaches zero, C_{i*} is the C_i-based CO_2 compensation point in the absence of R_d (by definition $C_{i*} = \Gamma_* - R_d/g_m$), and f_{vpd} is the function for the effect of leaf-to-air vapour pressure difference (VPD), which is not yet understood sufficiently and may be described empirically as:

$$f_{vpd} = \frac{1}{[1/(a_1 - b_1 VPD) - 1]} \qquad (15a)$$

where a_1 and b_1 are empirical constants. Eq. (15) is consistent with the finding that stomata may sense C_i [47]. Furthermore, unlike the model of Leuning et al. [16], Eq. (15) uses $(A + R_d)$ instead of A to avoid a possible negative g_s below the light compensation point. Unlike the model of Dewar [48], Eq. (15) predicts a non-zero g_s if $C_i = C_{i*}$. It also differs from the model of Tuzet et al. [46] in that there is no need to calculate Γ—the CO_2 compensation point in the presence of R_d.

The following equations can be written, according to Fick's first law of diffusion for CO_2 transfer along the path from C_a to C_c:

$$C_i = C_a - A \left(\frac{1}{g_b} + \frac{1}{g_s} \right) \qquad (16)$$

$$C_c = C_i - \frac{A}{g_m} \qquad (17)$$

The Rubisco-limited (A_c) and e$^-$ transport-limited (A_j) parts of the FvCB model can be written in a single equation as:

$$A = \frac{(C_c - \Gamma_*)x_1}{C_c + x_2} - R_d \qquad (18)$$

where for the Rubisco-limited part $x_1 = V_{cmax}$ and $x_2 = K_{mC}(1 + O/K_{mO})$, and for the e$^-$ transport-limited part $x_1 = J/4$ and $x_2 = 2\Gamma_*$.

Solving A from Eqs. (15)–(18) is commonly done by a numerical iteration approach (e.g., [16]). From applications in a large simulation framework such as for crop growth modelling, a faster approach is preferred. Here, an analytical approach is applied by combining and manipulating Eqs. (15)–(18) into the form of a standard cubic equation for A:

$$A^3 + pA^2 + qA + r = 0 \qquad (19)$$

The analytical solution for a general cubic equation is given in Appendix A. Lumped coefficients p, q, and r in Eq. (19) are given in Appendix B. The root A_1 in Appendix A was found to be suitable for calculating either A_c or A_j under any combinations of C_a, I_{inc}, temperature, and VPD. The minimum of A_c or A_j gives A according to Eq. (1).

5. The C$_4$ model

In C$_4$ plants, CO_2 is fixed initially in the mesophyll by phosphoenolpyruvate (PEP) carboxylase into C$_4$ acids that are then decarboxylated to supply CO_2 to Rubisco, which is localized in the bundle-sheath chloroplasts (Fig. 5). The well co-ordinated functioning of mesophyll and bundle-sheath cells, accomplished through specialized leaf anatomy, produces a high CO_2 concentration in the bundle sheath, strongly inhibiting photorespiration. However, the elevated CO_2 in the bundle-sheath cells is sustained at the cost of extra ATP, required for the regeneration of PEP.

The conductance for CO_2 transfer from intercellular air spaces to mesophyll cells may be large enough in C$_4$ leaves [49]. However, the bundle-sheath conductance (g_{bs}) is a major factor that determines the rate of CO_2 leakage from the bundle sheath to the mesophyll (L), and g_{bs} should be small enough for concentrating CO_2 in the bundle sheath. Following the model of von Caemmerer and Furbank [9], which was built upon several earlier models (e.g., [50]), the following two equations specific for C$_4$ photosynthesis can be written:

$$L = g_{bs}(C_c - C_i) \qquad (20a)$$

$$A = V_p - L - R_m \qquad (20b)$$

where V_p is the rate of PEP carboxylation, and R_m is the mitochondrial respiration occurring in the mesophyll, which for practical purposes can be set to $0.5R_d$. V_p can be limited either by the activity of PEP carboxylase or by the rate of e$^-$ transport. For the enzyme-limited case, von Caemmerer and Furbank [9] used a Michaelis–Menten equation to describe V_p. In order to find an analytical solution when combined with a g_s model, we use the version of Collatz et al. [51] and He and Edwards [52]:

$$V_p = \min(k_p C_i, V_{p\max}) \qquad (20c)$$

where k_p is the initial carboxylation efficiency of the PEP carboxylase, and V_{pmax} is the maximum rate of PEP carboxylation at the saturated C_i, the temperature response of which can be described by Eq. (6) [53]. Use of Eq. (20c) simplifies the model solution, but the
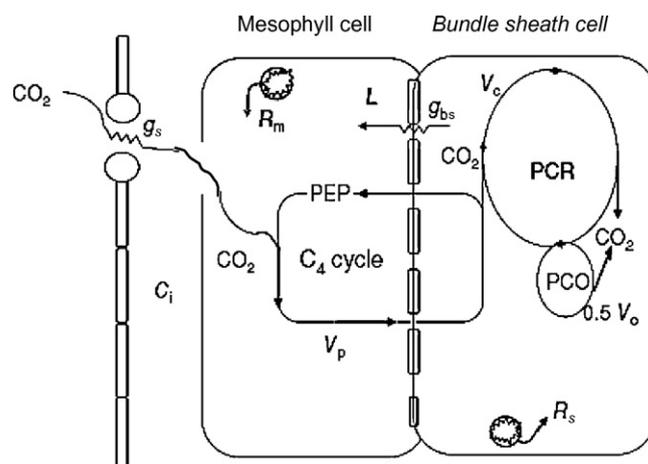
Fig. 5. Scheme of the C$_4$ photosynthesis model based on von Caemmerer and Furbank [9]. After passing the stomatal conductance (g_s) and entering the mesophyll cell, CO_2 is fixed by phosphoenolpyruvate (PEP) carboxylase at the rate of V_p. The formed C$_4$ acid crosses a bundle-sheath conductance (g_{bs}) and is decarboxylated at the same rate V_p. The released CO_2 either leaks back to the mesophyll cell (L) or can be fixed at the bundle-sheath cell by Rubisco at the rate V_c in the photosynthetic carbon reduction cycle (PCR – the normal C$_3$ cycle). Part of the CO_2 is again released by the photosynthetic carbon oxidation (PCO) cycle at half the rate of Rubisco oxygenation (V_o). CO_2 can also be released in the mesophyll and bundle sheath from mitochondrial respiration (R_m and R_s), which together make the total day respiration rate R_d.

modelled CO_2 response curve may reach saturation a little sooner than that given by using a Michaelis–Menten equation.

For the e^- transport-limited V_p, we use a generalized form (unpublished):

$$V_p(J_2) = \frac{xJ_2(2 + f_Q - f_{cyc})}{2h(1 - f_{cyc})} = \frac{xJ_2 z}{2} \qquad (20d)$$

where $z = (2 + f_Q - f_{cyc})/[h(1 - f_{cyc})]$; x represents the fraction of the total PSII e^- transport rate (J_2) partitioned to the mesophyll reactions, so $(1 - x)$ is the fraction of J_2 partitioned to the bundle-sheath reactions; the definition of the other variables in Eq. (20d) is the same as used for the C_3 generalized model, Eqs. (10a)–(10d).

Eqs. (20a) and (20b) can be combined to result in:

$$C_c = C_i + \frac{V_p - A - R_m}{g_{bs}} \qquad (21)$$

Incorporating algorithms from Eqs. (20c) and (20d), Eq. (21) can have different forms, depending on how V_p is calculated:

$$C_c = aC_i + \frac{b - A - R_m}{g_{bs}} \qquad (22)$$

where $a = \begin{cases} 1 + k_p/g_{bs} & \text{if} \quad V_p = k_p C_i \\ 1 & \text{if} \quad V_p = V_{pmax} \text{ or } V_p(J_2) \end{cases}$

and $b = \begin{cases} 0 & \text{if} \quad V_p = k_p C_i \\ V_{p\,max} & \text{if} \quad V_p = V_{p\,max} \\ V_p(J_2) & \text{if} \quad V_p = V_p(J_2) \end{cases}$.

As in C_3 photosynthesis, the rate of CO_2 fixation by Rubisco in C_4 photosynthesis can be limited either by the Rubisco activity (see Eq. (2)) or by the e^- transport. In combination, the net rate of CO_2 assimilation can be expressed as:

$$A = \frac{(C_c - \gamma_* O_{bs})x_1}{C_c + x_2 O_{bs} + x_3} - R_d \qquad (23)$$

where O_{bs} is the O_2 concentration in the bundle-sheath cell; $\gamma_* = 0.5/S_{c/o}$; $x_1 = V_{cmax}$, $x_2 = K_{mC}/K_{mO}$, $x_3 = K_{mC}$ for the enzyme (Rubisco)-limited rate, and $x_1 = (1 - x)J_2 z/3$, $x_2 = 7\gamma_*/3$ and $x_3 = 0$ for the e^- transport-limited rate (unpublished). This form of the e^- transport-limited rate implicitly assumes that it is the ATP supply rather than the NADPH supply that causes the e^- transport limitation in C_4 photosynthesis as a whole. This assumption holds because there is no net NADPH requirement by the C_4 cycle itself although in NADP-ME C_4 subtype, NADPH consumed in the production of malate is released in the bundle sheath during decarboxylation. However, there is the additional cost of 2 mol of ATP for the regeneration of 1 mol of PEP from pyruvate in the mesophyll [9].

In addition, PSII activity and O_2 evolution in the bundle sheath vary widely amongst the C_4 species. This has implications for the steady-state O_2 partial pressure of the bundle sheath. Following von Caemmerer and Furbank [9], a relation between intercellular air-space O_2 partial pressure (O_i) and the bundle-sheath O_2 partial pressure (O_{bs}) is described as:

$$O_{bs} = \frac{\alpha A}{0.047 g_{bs}} + O_i \qquad (24)$$

where α is the fraction of O_2 evolution occurring in the bundle sheath, and 0.047 accounts for the diffusivities for O_2 and CO_2 in water and their respective Henry constants [9]. For maize and sorghum, α will be zero whereas it will approach or even exceed 0.5 in other cases [54].

CO_2 transfer along the path from C_a to C_i is the same as in Eq. (16) for C_3 photosynthesis. However, to permit finding an analyti-

cal solution for A in C_4 photosynthesis, we use a slightly different phenomenological equation as a g_s model:

$$g_s = g_0 + \frac{A + R_d}{C_s - C_{s*}} f_{vpd} \qquad (25)$$

where C_s is the CO_2 level at leaf surface, and C_{s*} is the C_s-based CO_2 compensation point in the absence of R_d. By definition, C_{s*} and C_{i*} differ by $C_{s*} = C_{i*} - R_d/g_{s,C_{i*}}$, where $g_{s,C_{i*}}$ is the stomatal conductance at C_{i*}. The value of C_{i*} can be solved from Eqs. (21) and (24) with $C_c = \gamma_* O_{bs}$, $V_p = k_p C_{i*}$ and $A = -R_d$:

$$C_{i*} = \frac{g_{bs}\gamma_* O_i - (1 + \gamma_*\alpha/0.047)R_d + R_m}{g_{bs} + k_p} \qquad (26)$$

Combining Eqs. (16) and (22)–(25) and manipulating them can yield a form of cubic equation, Eq. (19), in which its coefficients are given in Appendix C. The root A_3 in Appendix A was found to be suitable for calculating A under any combination of C_a, I_{inc}, temperature, and VPD. As either the enzyme activity or the e^- transport can limit both Rubisco and PEP-carboxylase reactions, in theory four types of combinations of rate limitations are possible. The minimum of the four rates gives the prediction of A.

There is not published a simple calibration procedure as yet to account for alternative e^- transports and other uncertain factors as done for C_3 photosynthesis, see Eqs. (11)–(13). For C_4 photosynthesis, however, it is certain that the ATP supply causes the e^- transport limitation. Although non-chloroplastic processes (e.g., oxidative phosphorylation in mitochondria) could provide additional ATP in the PCK C_4 subtype, it is most likely that the high ATP requirement is largely met within the chloroplasts in the main C_4 crop species (maize and sorghum), since the respiration cost in C_4 leaves is generally not higher than in C_3 leaves [55]. An equation equivalent to Eq. (10d) for C_3 photosynthesis, can be derived for C_4 photosynthesis (unpublished):

$$1 - f_{cyc} - f_{pseudo} = \frac{(4C_c + 8\gamma_* O_{bs})(2 + f_Q - f_{cyc})(1 - x)}{h(3C_c + 7\gamma_* O_{bs})} \qquad (27)$$

Comparing Eq. (27) with Eq. (10d) shows that if f_Q and h were the same for C_3 and C_4 photosynthesis, the fraction for LET, i.e., $(1 - f_{cyc} - f_{pseudo})$ (see Fig. 3), would need to be decreased in C_4 photosynthesis by a factor $(1 - x)$. To meet the high demand for ATP in C_4 photosynthesis, however, the Q-cycle, an efficient proton-pumping routine along the LET chain (Fig. 3), is obligatory [56]. So f_Q is set to 1. As there are minor physiological processes simultaneously occurring with CO_2 fixation that consume e^- or reductants from the chloroplasts [57,58], the value of f_{pseudo} can be practically assigned, e.g., ca. 0.1 for both C_3 [35] and C_4 plants [59], but with caution as the exact value of f_{pseudo} is unknown. These minor physiological processes are beyond the scope of modelling photosynthesis in this paper and are not described in detail. Assuming photorespiration is negligible in C_4 leaves, the required f_{cyc} can be solved from Eq. (27) as:

$$f_{cyc} = 1 - \frac{4(1 - x)(1 + f_Q) + 3hf_{pseudo}}{3h - 4(1 - x)} \qquad (28)$$

where x may be set at 0.4, based on an optimization analysis for a wide range of conditions ([9]; and references therein). There is uncertainty about the value of parameter h (3, 4 or 14/3), which has been debated for C_3 photosynthesis [35,54]. Eq. (28) predicts that f_{cyc} is 0.136, 0.375 and 0.466 if h is 3, 4 and 14/3, respectively. When f_{cyc} is known, the required J_2, see Eqs. (20d) and (23), can be calculated using Eqs. (10b) and (10c). Although simulation shows that C_c can be low enough (Fig. 6) for small photorespiration to occur at limiting light levels, simulated values for $\Phi_{CO_2(LL)}$ using the above assumptions agree with the range of measured $\Phi_{CO_2(LL)}$ for C_4 species [37,60,61], with $h = 3$ giving $\Phi_{CO_2(LL)}$ at the upper side and $h = 14/3$ giving a value at the lower side of the range. However,

the reported interspecific difference in $\Phi_{CO_2(LL)}$ could be due to the variation in other parameters (e.g., g_{bs}). Furthermore, it is unclear whether the chloroplasts are flexible enough (e.g., via state transition) to support CET with a high f_{cyc} close to or even above 0.4. Thus, for the following section we use the conservative value for h (i.e., 3), which was previously assumed to assess quantum requirement of C_4 photosynthesis (e.g., [50,56]), but with the caution that h is likely to be 4.

6. Simulation highlights and some remarks from the perspective of crop modelling

Some constants characterizing temperature response of enzyme kinetics are not yet well quantified for C_4 photosynthesis (Table 2). However, in addition to those for C_3 photosynthesis, the most important algorithms for C_4 photosynthesis are the ones that capture the CO_2 concentrating mechanism and the extra ATP requirement by the PEP regeneration. Fig. 6 compares the level of the simulated C_c in C_3 and C_4 leaves as a function of irradiance. At high light levels, C_c of C_4 leaves is 8–10 times that of C_3 leaves, which largely explains why there is virtually no photorespiration in C_4 leaves. At low light levels, the difference is smaller, due to a higher fraction of leakage of CO_2 back to the mesophyll cell. As a result, the predicted light response curve saturates at a much higher light level, the predicted CO_2 response curve saturates at a much lower CO_2 level, and the predicted temperature response curve has a higher temperature optimum in C_4 than C_3 photosynthesis (Fig. 7), whereas the predicted difference in the photosynthetic quantum efficiency $\Phi_{CO_2(LL)}$ at a reference 25 °C is relatively small (Fig. 8). We emphasize that the modelled differences in response curves and values of $\Phi_{CO_2(LL)}$ between C_3 and C_4 cases should not be considered as absolute as we only used default parameter values to illustrate general trends. Overall, C_4 photosynthesis response curves are very similar to those for C_3 photosynthesis measured under low O_2 or/and high CO_2 conditions (which can suppress
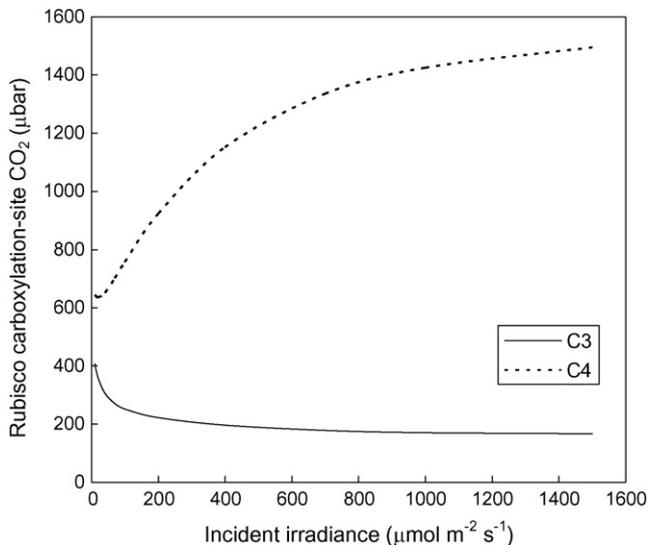
Fig. 6. Comparison of simulated CO_2 partial pressure at the Rubisco carboxylation site between C_3 and C_4 leaves. For this simulation, $C_a = 360$ μbar, $T = 25$ °C, VPD = 2.1 kPa, $O_i = 210{,}000$ μbar, $V_{cmax25} = 120$ μmol m^{-2} s^{-1}, $J_{max25} = 230$ μmol m^{-2} s^{-1}, $R_{d25} = 0.01 V_{cmax25}$, $g_b = 1.5$ mol m^{-2} s^{-1} bar^{-1}, $g_0 = 0.01$ mol m^{-2} s^{-1} bar^{-1}, $a_1 = 0.9$, $b_1 = 0.15$ kPa^{-1}. For C_3: $g_m = 0.4$ mol m^{-2} s^{-1} bar^{-1}; for C_4: $\alpha = 0.1$; $g_{bs} = 0.003$ mol m^{-2} s^{-1} bar^{-1}. For C_4 simulation, the small difference between C_{s*} and C_{i*} was assumed negligible; furthermore, V_{pmax} was tentatively assumed not limiting on V_p because how it scales quantitatively with V_{cmax} or with J_{max} is not yet very clear; but this assumption has very little impact on the general conclusions of this and subsequent simulations because with increasing C_i, $V_p(J_2)$ will soon replace k_pC_i to become limiting on V_p.
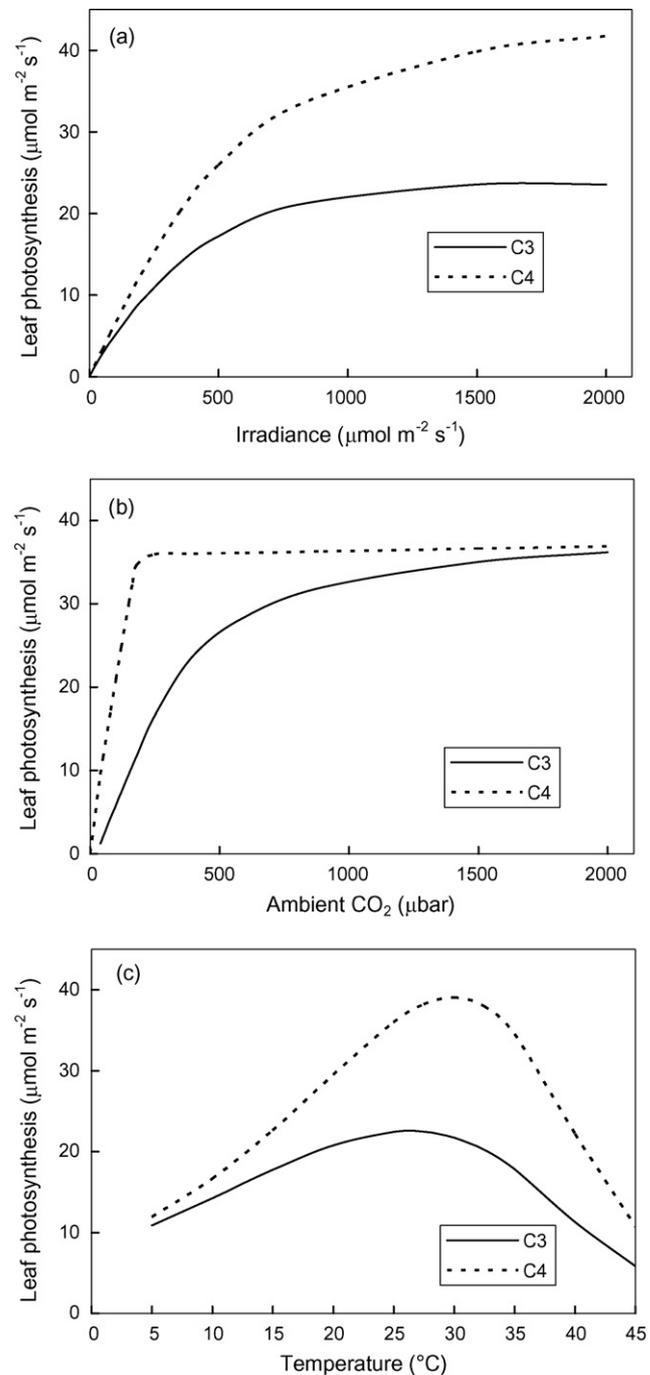
Fig. 7. Simulated curves of C_3 and C_4 gross photosynthesis in response to irradiance where $C_a = 360$ μbar and $T = 25$ °C (a), to ambient CO_2 where $I_{inc} = 1000$ μmol m^{-2} s^{-1} and $T = 25$ °C (b), and to temperatures where $I_{inc} = 1000$ μmol m^{-2} s^{-1} and $C_a = 360$ μbar (c). Model constants used for this simulation are shown in Table 2; for other parameters see Fig. 6.

photorespiration), except that $\Phi_{CO_2(LL)}$ in C_4 leaves is significantly lower than $\Phi_{CO_2(LL)}$ in C_3 leaves under the non-photorespiratory condition, the latter having a value of 0.09–0.11 [37,62].

As stated earlier, $\Phi_{CO_2(LL)}$ is an important parameter for the photosynthetic light response curve in many crop growth models. Our model algorithms predict that at a C_a of 360 μbar, $\Phi_{CO_2(LL)}$ decreases sharply with increasing temperature in C_3 plants but remains virtually insensitive to temperature in C_4 plants (Fig. 9a), consistent with experimental evidence [60,61]. The predicted sensitivity of $\Phi_{CO_2(LL)}$ to temperature for C_3 plants at a doubled CO_2
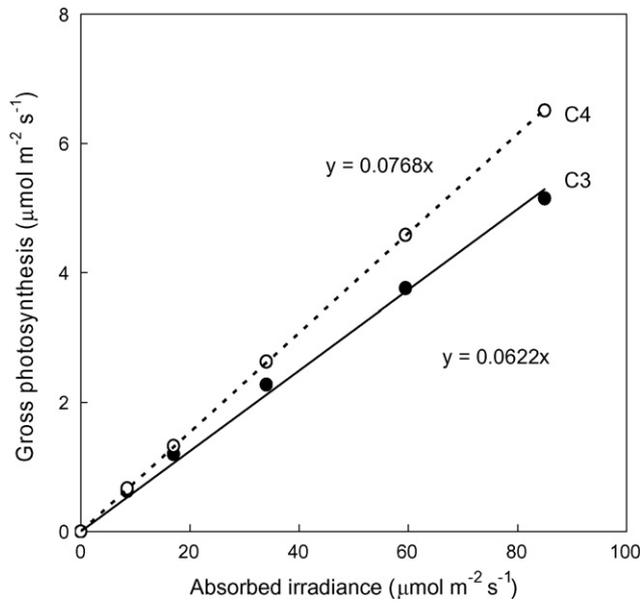
Fig. 8. Illustration of the calculation of photosynthetic quantum efficiency at limiting light levels ($\Phi_{CO_2(LL)}$) using simulated gross CO_2 assimilation rates $A + R_d$ (points). $C_a = 360\,\mu$bar and $T = 25\,°$C. The slope of the linear regression through the origin is $\Phi_{CO_2(LL)}$. Model constants used for this simulation are shown in Table 2; for other parameters see Fig. 6.

level is reduced, compared with the response under the ambient CO_2 condition (Fig. 9a). This is supported by the experimental measurement of Ku and Edwards [63] that the sensitivity of $\Phi_{CO_2(LL)}$ to temperature in wheat is reduced by a reduced O_2 level. To quantify the interaction between the effect of temperature, $f(T)$, and the effect of C_a, $g(C_a)$, on $\Phi_{CO_2(LL)}$, the rice growth model ORYZA [31] uses the following empirical, multiplicative expression:

$$\Phi_{CO_2(LL)} = \Phi_{CO_2(LL)ref} f(T) g(C_a) \tag{29}$$

where $\Phi_{CO_2(LL)ref}$ is $\Phi_{CO_2(LL)}$ at a reference temperature and C_a; and $f(T)$ and $g(C_a)$ were established from separate experimental data. This model predicts an increased temperature sensitivity of $\Phi_{CO_2(LL)}$ under the elevated CO_2 condition (Fig. 9b). The earlier version of the ORYZA model was used to assess the impact of global warming on the Asian rice production [64]. It is clear that its simulation results should receive a critical reservation because the underlying sub-model for photosynthesis does not predict correctly (1) the temperature optimum shift and the temperature range (within which A is positive) at elevated CO_2 (Fig. 2) and (2) the direction of interaction between temperature and elevated CO_2 on $\Phi_{CO_2(LL)}$ (Fig. 9).

Multiplicative models like Eq. (29) have often been used by crop modellers as a standard method to describe how physiological processes respond to two or more interacting variables. The example shown in Fig. 9 means that this form can be incorrect. Algorithms in major crop growth models have been updated little since the late 1980s, indicating "a sense of arrogance and complacency" [65]. To face new challenges in crop science, crop modellers should be willing to utilize the rich knowledge at a lower scale, such as elegant yet simple FvCB-type photosynthesis models already available for years. A common view of crop modellers is that parameterization of the FvCB model for different crops is difficult and time-consuming [66]. Given the increasing availability of a wealth of information for the key enzyme constants (Table 2), which are believed to be conservative among C_3 or C_4 species, the task of parameterization can focus on a few key parameters, estimated by curve fitting to readily available gas exchange measurements (e.g., [17,19]). The version of C_3 and C_4 photosynthesis models presented here has just
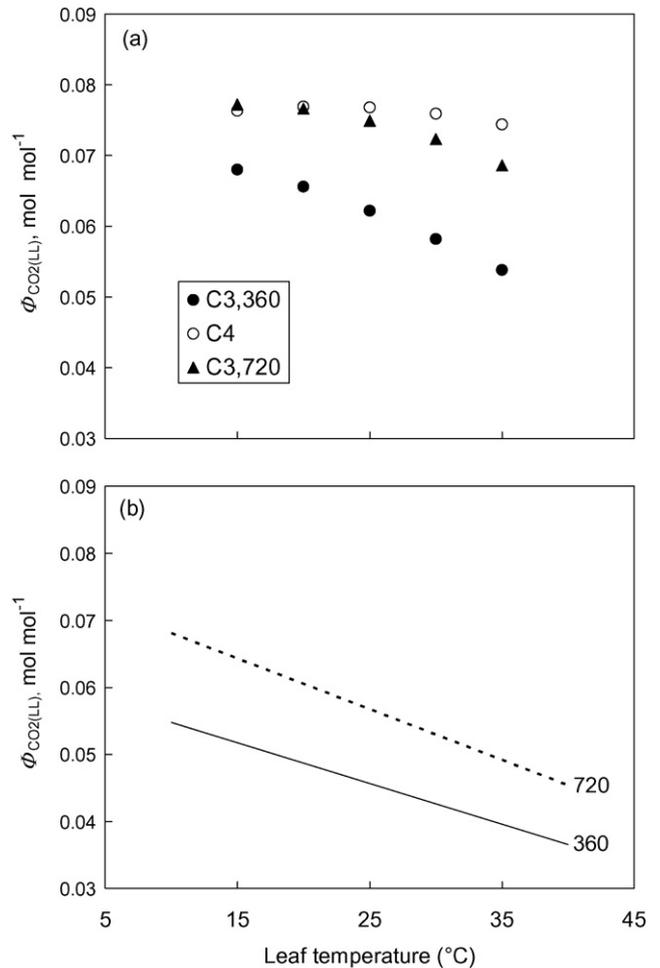
Fig. 9. Temperature response of photosynthetic quantum efficiency under limiting lights $\Phi_{CO_2(LL)}$, simulated by the C_3 and C_4 models described here (a), or by the empirical multiplicative Eq. (29) as used in the ORYZA model [31] (b). For the C_3 case in both panels, two levels of C_a (360 and 720 μbar) were considered, whereas for the C_4 case shown in panel (a), $C_a = 360\,\mu$bar. Model constants used for simulation shown in panel (a) are given in Table 2; for other parameters see Fig. 6.

been incorporated into a relatively new crop growth model GECROS [24]. This model allows one to objectively examine a number of important research questions, such as exploring options for bio-energy production and assessing impacts of global warming and transformation of C_4 routine into C_3 crops on season-long canopy photosynthesis and crop grain yields. Crop modelling has been by and large reliant on simple approaches; however, in the words attributed to Albert Einstein, "*Everything should be made as simple as possible, but not simpler*".

Appendix A. Analytical solution of a cubic equation—Eq. (19)

The solution of the standard form of a cubic equation like Eq. (19) is taken from Press et al. [67]; see also Collatz et al. [51] and Baldocchi [68]. Three roots for the equation are:

$$A_1 = -2\sqrt{Q}\cos\left(\frac{\psi}{3}\right) - \frac{p}{3}$$

$$A_2 = -2\sqrt{Q}\cos\left(\frac{\psi + 2\pi}{3}\right) - \frac{p}{3}$$

$$A_3 = -2\sqrt{Q}\cos\left(\frac{\psi + 4\pi}{3}\right) - \frac{p}{3}$$

where $Q = (p^2 - 3q)/9$; $\quad \psi = \arccos(U/\sqrt{Q^3})$; $U = (2p^3 - 9pq + 27r)/54$.

Appendix B. Lumped coefficients in Eq. (19) for the coupled C$_3$ photosynthesis and diffusional conductance model

The coefficients p, q and r of Eq. (19) for C$_3$ photosynthesis are:

$$p = -\frac{[d + (x_1 - R_d)/g_m + a(1/g_m + 1/g_b) + (g_0/g_m + f_{vpd})c]}{m}$$

$$q = \frac{[d(x_1 - R_d) + ac + (g_0/g_m + f_{vpd})b]}{m}$$

$$r = -\frac{ab}{m}$$

where the coefficients a, b, c, d and m are expressed as:

$$a = g_0(x_2 + \Gamma_*) + \left(\frac{g_0}{g_m} + f_{vpd}\right)(x_1 - R_d)$$

$$b = C_a(x_1 - R_d) - \Gamma_* x_1 - R_d x_2$$

$$c = C_a + x_2 + \left(\frac{1}{g_m} + \frac{1}{g_b}\right)(x_1 - R_d)$$

$$d = x_2 + \Gamma_* + \frac{(x_1 - R_d)}{g_m}$$

$$m = \frac{1}{g_m} + \left(\frac{g_0}{g_m} + f_{vpd}\right)\left(\frac{1}{g_m} + \frac{1}{g_b}\right)$$

where x_1 and x_2 are defined in the texts following Eq. (18).

Appendix C. Lumped coefficients in Eq. (19) for the coupled C$_4$ photosynthesis and diffusional conductance model

The coefficients p, q and r of Eq. (19) for C$_4$ photosynthesis are:

$$p = \frac{[j - (h - lR_d)]}{l}$$

$$q = \frac{(i + jR_d - g)}{l}$$

$$r = -\frac{(f - iR_d)}{l}$$

where the coefficients f, g, h, i, j and l are expressed as:

$$f = (b - R_m - \gamma_* O_i g_{bs})x_1 d + a g_{bs} x_1 C_a d$$

$$g = (b - R_m - \gamma_* O_i g_{bs})x_1 m - \left(\frac{\alpha \gamma_*}{0.047} + 1\right)x_1 d$$
$$+ a g_{bs} x_1 \left[C_a m - \frac{d}{g_b} - (C_a - C_{s*})\right]$$

$$h = -\left[\left(\frac{\alpha \gamma_*}{0.047} + 1\right)x_1 m + \frac{a g_{bs} x_1(m-1)}{g_b}\right]$$

$$i = (b - R_m + g_{bs}x_3 + x_2 g_{bs}O_i)d + a g_{bs} C_a d$$

$$j = (b - R_m + g_{bs}x_3 + x_2 g_{bs}O_i)m + \left(\frac{\alpha x_2}{0.047} - 1\right)d$$
$$+ a g_{bs}\left[C_a m - \frac{d}{g_b} - (C_a - C_{s*})\right]$$

$$l = \left(\frac{\alpha x_2}{0.047} - 1\right)m - \frac{a g_{bs}(m-1)}{g_b}$$

where x_1, x_2 and x_3 are defined in the texts following Eq. (23), a and b are defined in the equations below Eq. (22), and d and m are defined as:

$$d = g_0 C_a - g_0 C_{s*} + f_{vpd}R_d$$

$$m = f_{vpd} - \frac{g_0}{g_b}$$

References

[1] A. Laisk, H. Eichelmann, V. Oja, C$_3$ photosynthesis in silico, Photosynthesis Research 90 (2006) 45–66.

[2] X.-G. Zhu, E. de Sturler, S.P. Long, Optimizing the distribution of resources between enzymes of carbon metabolism can dramatically increase photosynthetic rate: a numerical simulation using an evolutionary algorithm, Plant Physiology 145 (2007) 513–526.

[3] G.D. Farquhar, S. von Caemmerer, J.A. Berry, A biochemical model of photosynthetic CO$_2$ assimilation in leaves of C$_3$ species, Planta 149 (1980) 78–90.

[4] S. von Caemmerer, G.D. Farquhar, Some relationships between the biochemistry of photosynthesis and the gas exchange of leaves, Planta 153 (1981) 376–387.

[5] S. von Caemmerer, J.R. Evans, G.S. Hudson, T.J. Andrews, The kinetics of ribulose-1,5-bisphosphate carboxylase/oxygenase in vivo inferred from measurements of photosynthesis in leaves of transgenic tobacco, Planta 195 (1994) 88–97.

[6] C.J. Bernacchi, A.R. Portis, H. Nakano, S. von Caemmerer, S.P. Long, Temperature response of mesophyll conductance. Implication for the determination of Rubisco enzyme kinetics and for limitations to photosynthesis in vivo, Plant Physiology 130 (2002) 1992–1998.

[7] S.P. Long, Modification of the response of photosynthetic productivity to rising temperature by atmospheric CO$_2$ concentrations: has its importance been underestimated? Plant, Cell and Environment 14 (1991) 729–739.

[8] J. Lloyd, G.D. Farquhar, The CO$_2$ dependence of photosynthesis, plant growth responses to elevated atmospheric CO$_2$ concentrations and their interactions with soil nutrient status. II. Temperate and boreal forest productivity and the combined effects of increased CO$_2$ concentrations and increased nitrogen deposition at a global scale, Functional Ecology 13 (1999) 439–459.

[9] S. von Caemmerer, R.T. Furbank, Modeling C$_4$ photosynthesis, in: R.F. Sage, R.K. Monson (Eds.), C$_4$ Plant Biology, Academic Press, Toronto, 1999, pp. 173–211.

[10] T.D. Sharkey, M. Stitt, D. Heineke, R. Gerhardt, K. Raschke, H.W. Heldt, Limitation of photosynthesis by carbon metabolism. II. O$_2$-insensitive CO$_2$ uptake results from limitation of triose phosphate utilization, Plant Physiology 81 (1986) 1123–1129.

[11] G.D. Farquhar, S. von Caemmerer, Modelling of photosynthetic response to environmental conditions, in: O.L. Lange, P.S. Nobel, C.B. Osmond, H. Ziegler (Eds.), Physiological Plant Ecology II, Water Relations and Carbon Assimilation. Encyclopaedia of Plant Physiology, New Series, vol. 12B, Springer-Verlag, Berlin, 1982, pp. 549–588.

[12] G.D. Farquhar, S.C. Wong, An empirical model of stomatal conductance, Australian Journal of Plant Physiology 11 (1984) 191–210.

[13] M. Kasahara, T. Kagawa, K. Olkawa, N. Suetsugu, M. Miyao, M. Wada, Chloroplast avoidance movement reduces photodamage in plants, Nature 420 (2002) 829–832.

[14] P.C. Harley, R.B. Thomas, J.F. Reynolds, B.R. Strain, Modelling photosynthesis of cotton grown in elevated CO$_2$, Plant, Cell and Environment 15 (1992) 271–282.

[15] S.D. Wullschleger, Biochemical limitations to carbon assimilation in C$_3$ plants – a retrospective analysis of the A/C_i curves from 109 species, Journal of Experimental Botany 44 (1993) 907–920.

[16] R. Leuning, F.M. Kelliher, D.G.G. De Pury, E.-D. Schulze, Leaf nitrogen, photosynthesis, conductance and transpiration: scaling from leaves to canopies, Plant, Cell and Environment 18 (1995) 1183–1200.

[17] B.E. Medlyn, E. Dreyer, D. Ellsworth, M. Forstreuter, P.C. Harley, M.U.F. Kirschbaum, X. Le Roux, P. Montpied, J. Strassemeyer, A. Walcroft, K. Wang, D. Loustau, Temperature response of parameters of a biochemically based model of photosynthesis. II. A review of experimental data, Plant, Cell and Environment 25 (2002) 1167–1179.

[18] T. June, J.R. Evans, G.D. Farquhar, A simple new equation for the reversible temperature dependence of photosynthetic electron transport: a study on soybean leaf, Functional Plant Biology 31 (2004) 275–283.

[19] X. Yin, M. van Oijen, A.H.C.M. Schapendonk, Extension of a biochemical model for the generalized stoichiometry of electron transport limited C$_3$ photosynthesis, Plant, Cell and Environment 27 (2004) 1211–1222.

[20] X. Yin, P.C. Struik, P. Romero, J. Harbinson, J.B. Evers, P.E.L. van der Putten, J. Vos, Using combined measurements of gas exchange and chlorophyll fluorescence to estimate parameters of a biochemical C_3 photosynthesis model: a critical appraisal and a new integrated approach applied to leaves in a wheat (*Triticum aestivum*) canopy, Plant, Cell and Environment 32 (2009) 448–464.

[21] S.E. Taylor, N. Terry, Limiting factors in photosynthesis. V. Photochemical energy supply colimits photosynthesis at low values of intercellular CO_2 concentration, Plant Physiology 75 (1984) 82–86.

[22] A. Brooks, G.D. Farquhar, Effect of temperature on the CO_2/O_2 specificity of ribulose-1,5-bisphosphate carboxylase/oxygenase and the rate of respiration in the light, Planta 165 (1985) 397–406.

[23] B.E. Medlyn, F.-W. Badeck, D.G.G. De Pury, C.V.M. Barton, M. Broadmeadow, R. Ceulemans, P. De Angelis, M. Forstreuter, M.E. Jach, S. Kellomäki, E. Laitat, M. Marek, S. Philippot, A. Rey, J. Strassemeyer, K. Laitinen, R. Liozon, B. Portier, P. Roberntz, K. Wang, P.G. Jstbid, Effects of elevated [CO_2] on photosynthesis in European forest species: a meta-analysis of model parameters, Plant, Cell and Environment 22 (1999) 1475–1495.

[24] X. Yin, H.H. van Laar, Crop Systems Dynamics: An Ecophysiological Simulation Model for Genotype-by-Environment Interactions, Wageningen Academic Publishers, Wageningen, The Netherlands, 2005.

[25] S.P. Long, C.J. Bernacchi, Gas exchange measurements, what can they tell us about the underlying limitations to photosynthesis? Procedures and sources of error, Journal of Experimental Botany 54 (2003) 2393–2401.

[26] G.J. Ethier, N.J. Livingston, D.L. Harrison, T.A. Black, J.A. Moran, Low stomatal and internal conductance to CO_2 versus Rubisco deactivation as determinants of the photosynthetic decline of ageing evergreen leaves, Plant, Cell and Environment 29 (2006) 2168–2184.

[27] J.-J.B. Dubois, E.L. Fiscus, F.L. Booker, M.D. Flowers, C.D. Reid, Optimizing the statistical estimation of the parameters of the Farquhar-von Caemmerer-Berry model of photosynthesis, New Phytologist 176 (2007) 402–414.

[28] T.D. Sharkey, C.J. Bernacchi, G.D. Farquhar, E.L. Singsaa, Fitting photosynthetic carbon dioxide response curves for C_3 leaves, Plant, Cell and Environment 30 (2007) 1035–1040.

[29] M. van Oijen, M.F. Dreccer, K.-H. Firsching, B.J. Schnieders, Simple equations for dynamic models of the effects of CO_2 and O_3 on light use efficiency and growth of crops, Ecological Modelling 179 (2004) 39–60.

[30] K.J. Boote, N.B. Pickering, Modeling photosynthesis of row crop canopies, HortScience 29 (1994) 1423–1434.

[31] B.A.M. Bouman, M.J. Kropff, T.P. Tuong, M.C.S. Wopereis, H.F.M. ten Berge, H.H. van Laar, ORYZA2000: modelling lowland rice. International Rice Research Institute, Los Baños, The Philippines, and Wageningen University and Research Centre, The Netherlands, 2001.

[32] R.R. Wise, A.J. Olson, S.M. Schrader, T.D. Sharkey, Electron transport is the functional limitation of photosynthesis in field-grown Pima cotton plants at high temperature, Plant, Cell and Environment 27 (2004) 717–724.

[33] J.F. Allen, Cyclic, pseudocyclic and noncyclic photophosphorylation: new links in the chain, Trends in Plant Science 8 (2003) 15–19.

[34] T.J. Avenson, A. Kanazawa, J.A. Cruz, K. Takizawa, W.E. Ettinger, D.M. Kramer, Integrating the proton circuit into photosynthesis: progress and challenges, Plant, Cell and Environment 28 (2005) 97–109.

[35] X. Yin, J. Harbinson, P.C. Struik, Mathematical review of literature to assess alternative electron transports and interphotosystem excitation partitioning of steady-state C_3 photosynthesis under limiting light, Plant, Cell and Environment 29 (2006) 1771–1782 (with corrigendum in Plant, Cell and Environment 29: 2252).

[36] H.-W. Trissl, C. Wilhelm, Why do thylakoid membranes from higher plants form grana stacks? Trends in Biochemical Sciences 18 (1993) 415–419.

[37] O. Björkman, B. Demmig, Photon yield of O_2 evolution and chlorophyll fluorescence characteristics at 77 K among vascular plants of diverse origins, Planta 170 (1987) 489–504.

[38] C.J. Bernacchi, C. Pimentel, S.P. Long, *In vivo* temperature response functions of parameters required to model RuBP-limited photosynthesis, Plant, Cell and Environment 26 (2003) 1419–1430.

[39] J. Flexas, M. Ribas-Carbó, A. Diaz-Espejo, J. Galmes, H. Medrano, Mesophyll conductance to CO_2: current knowledge and future prospects, Plant, Cell and Environment 31 (2008) 602–621.

[40] C.R. Warren, Estimating the internal conductance to CO_2 movement, Functional Plant Biology 33 (2006) 431–442.

[41] T.L. Pons, J. Flexas, S. von Caemmerer, J.R. Evans, B. Genty, M. Ribas-Carbo, E. Brugnoli, Estimating mesophyll conductance to CO_2: methodology, potential errors, and recommendations, Journal of Experimental Botany 60 (2009) 2217–2234.

[42] X. Yin, P.C. Struik, Theoretical reconsiderations when estimating the mesophyll conductance to CO_2 diffusion in leaves of C_3 plants by analysis of combined gas exchange and chlorophyll fluorescence measurements. Plant, Cell and Environment, in press, doi:10.1111/j.1365-3040.2009.02016.x.

[43] C.R. Warren, E. Dreyer, Temperature response of photosynthesis and internal conductance to CO_2: results from two independent approaches, Journal of Experimental Botany 57 (2006) 3057–3067.

[44] W. Yamori, K. Noguchi, Y.T. Hanba, I. Terashima, Effects of internal conductance on the temperature dependence of the photosynthetic rate in spinach leaves from contrasting growth temperatures, Plant and Cell Physiology 47 (2006) 1069–1080.

[45] J. Flexas, A. Diaz-Espejo, J. Galmes, R. Kaldenhoff, H. Medrano, M. Ribas-Carbó, Rapid variation of mesophyll conductance in response to changes in CO_2 concentration around leaves, Plant, Cell and Environment 30 (2007) 1284–1298.

[46] A. Tuzet, A. Perrier, R. Leuning, A coupled model of stomatal conductance, photosynthesis and transpiration, Plant, Cell and Environment 26 (2003) 1097–1116.

[47] K.A. Mott, Do stomata respond to CO_2 concentrations other than intercellular? Plant Physiology 86 (1988) 200–203.

[48] R.C. Dewar, The Ball-Berry-Leuning and Tardieu-Davies stomatal models: synthesis and extension within a spatially aggregated picture of guard cell function, Plant, Cell and Environment 25 (2002) 1383–1398.

[49] M. Pfeffer, M. Peisker, CO_2 exchange and phosphoenolpyruvate carboxylase activity in leaves of *Zea mays* L., Photosynthesis Research 58 (1998) 281–291.

[50] G.D. Farquhar, On the nature of carbon isotope discrimination in C_4 species, Australian Journal of Plant Physiology 10 (1983) 205–226.

[51] G.J. Collatz, M. Ribas-Carbo, J.A. Berry, Coupled photosynthesis-stomatal conductance model for leaves of C_4 plants, Australian Journal of Plant Physiology 19 (1992) 519–538.

[52] D. He, G.E. Edwards, Estimation of diffusive resistance of bundle sheath cells to CO_2 from modeling of C4 photosynthesis, Photosynthesis Research 49 (1996) 195–208.

[53] R.-S. Massad, A. Tuzet, O. Bethenod, The effect of temperature on C_4-type leaf photosynthesis parameters, Plant, Cell and Environment 30 (2007) 1191–1204.

[54] S. von Caemmerer, Biochemical Models of Leaf Photosynthesis. Techniques in Plant Sciences No. 2, CSIRO Publishing, Collingwood, Victoria, Australia, 2000.

[55] G.T. Byrd, R.F. Sage, R.H. Brown, A comparison of dark respiration between C_3 and C_4 plants, Plant Physiology 100 (1992) 191–198.

[56] R.T. Furbank, C.L.D. Jenkins, M.D. Hatch, C_4 photosynthesis: quantum requirement, C_4 acid overcycling and Q-cycle involvement, Australian Journal of Plant Physiology 17 (1990) 1–7.

[57] J.P. Krall, R.W. Pearcy, Concurrent measurements of oxygen and carbon dioxide exchange during lightflecks in maize (*Zea mays* L.), Plant Physiology 103 (1993) 823–828.

[58] G. Noctor, C.H. Foyer, A re-evaluation of the ATP:NADPH budget during C_3 photosynthesis: a contribution from nitrate assimilation and its associated respiratory activity? Journal of Experimental Botany 49 (1998) 1895–1908.

[59] A. Laisk, G.E. Edwards, A mathematical model of C_4 photosynthesis: the mechanism of concentrating CO_2 in NADP-malic enzyme type species, Photosynthesis Research 66 (2000) 199–224.

[60] R.K. Monson, R.O. Littlejohn Jr., G.J. Williams III, The quantum yield for CO_2 uptake in C_3 and C_4 grasses, Photosynthesis Research 3 (1982) 153–159.

[61] J. Ehleringer, R.W. Pearcy, Variation in quantum yield for CO_2 uptake among C_3 and C_4 plants, Plant Physiology 73 (1983) 555–559.

[62] S.P. Long, W.F. Postl, H.R. Bolhár-Nordenkampf, Quantum yields for uptake of carbon dioxide in C_3 vascular plants of contrasting habitats and toxonomic groupings, Planta 189 (1993) 226–234.

[63] S.-B. Ku, G.E. Edwards, Oxygen inhibition of photosynthesis. III. Temperature dependence of quantum yield and its relation to O_2/CO_2 solubility ratio, Planta 140 (1978) 1–6.

[64] R.B. Matthews, M.J. Kropff, T. Horie, D. Bachelet, Simulating the impact of climate change on rice production in Asia and evaluating options for adaptation, Agricultural Systems 54 (1997) 399–425.

[65] A. Weiss, Introduction, Agronomy Journal 95 (2003) 1–3.

[66] F.N. Tubiello, F. Ewert, Simulating the effects of elevated CO_2 on crops: approaches and applications for climate change, European Journal of Agronomy 18 (2002) 57–74.

[67] W.H. Press, B.P. Flannery, S.A. Teukolsky, W.T. Vetterling, Numerical Recipes: The Art of Scientific Computing, Cambridge University Press, Cambridge, UK, 1989.

[68] D. Baldocchi, An analytical solution for coupled leaf photosynthesis and stomatal conductance models, Tree Physiology 14 (1994) 1069–1079.

[69] K. Asada, The water-water cycle as alternative photon and electron sinks, Philosophical Transactions of the Royal Society of London, Series B, Biological Sciences 355 (2000) 1419–1431.

[70] X. Yin, J. Harbinson, P.C. Struik, A model of the generalized stoichiometry of electron transport-limited C_3 photosynthesis. Development and Applications, in: A. Laisk, L. Nedbal, Govindjee (Eds.), Photosynthesis *in silico*: Understanding Complexity from Molecules to Ecosystems, vol. 29, Book series 'Advances in Photosynthesis and Respiration', Springer, The Netherlands (2009) 247–273.

[71] C.J. Bernacchi, E.L. Singsaas, C. Pimentel, A.R. Portis Jr., S.P. Long, Improved temperature response functions for models of Rubisco-limited photosynthesis, Plant, Cell and Environment 24 (2001) 253–259.

[72] A.H. Kingston-Smith, J. Harbinson, C.H. Foyer, Acclimation of photosynthesis, H_2O_2 content and antioxidants in maize (*Zea mays*) grown at sub-optimal temperatures, Plant, Cell and Environment 22 (1999) 1071–1083.

[73] J.R. Evans, Photosynthetic acclimation and nitrogen partitioning within a lucerne canopy. II. Stability through time and comparison with a theoretical optimum, Australian Journal of Plant Physiology 20 (1993) 69–82.

[74] J.I.L. Morison, R.M. Gifford, Stomatal sensitivity to carbon dioxide and humidity, Plant Physiology 71 (1983) 789–796.